Molecular Cell, Volume *32*

Supplemental Data

Small-Molecule Inhibitors of HIF-2a

Translation Link Its 5′-UTR Iron-Responsive

Element to Oxygen Sensing

Michael Zimmer, Benjamin L. Ebert, Christopher Neil, Keith Brenner, Ioannis Papaioannou, Antonia Melas, Nicola Tolliday, Justin Lamb, Kostas Pantopoulos, Todd Golub, and Othon Iliopoulos

Figure S1. Description and validation of luciferase reporter constructs. (a) *Schematic of HRE luciferase reporter constructs*. (b) *Fold induction of pGL3::HRE reporter constructs by cobalt chloride and desferrioxamine*. pGL3 derived reporter constructs were transiently transfected into U2OS cells and cobalt chloride ($CoCl_2$, 150 µM) or desferrioxamine (DFO, 150 µM) was added after 16 hours. Cells were harvested at 24 hours and measured for normalized luciferase activity. Shown is the fold increase over baseline for each reporter construct. *Gray bars*, $CoCl_2$; *open bars*, DFO. (c) *HRE4-luciferase reporter activity is inhibited by dominant negative HIF-2a mutants*. pGL3::HRE4 was transiently transfected into U2OS cells alone (lane 1) or with HIF-2a (P531A) (lanes 2-11), in the presence of increasing amounts of three dominant negative HIF-2a constructs, dnHIF-2a A (lanes 3-5), B (lanes 5-8) and C (lanes 9-11). (d) *Response of subcloned reporter constructs to hypoxia and hypoxia mimetics*. U2OS cells were transiently transfected with pcDNA3.1::SV40 (*gray bars*) or pCDNA3.1::HRE4 (*open bars*) plasmids and co-transfected with HIF-2a (P531A) mutant, stimulated by the hypoxia mimetics DFO or $CoCl_2$ for 12 hours, or subjected to hypoxia for 24 hours. Shown is the fold increase over baseline for each reporter construct. All experiments were performed in triplicate. Error bars represent standard error of the mean (SEM).

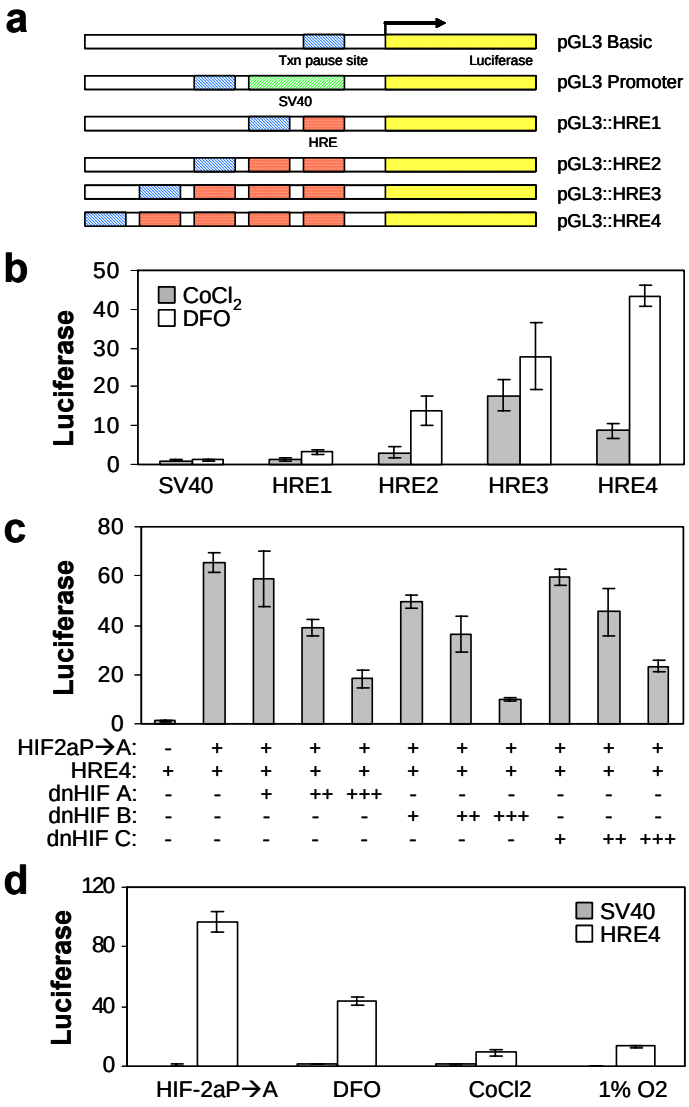

Figure S2. Compounds affect multiple RCC cell lines. Compounds were tested on stable polyclonal versions of VHL-defective lines expressing either the SV40- or HRE-luciferase reporter constructs. (a) A498, (b) UOK121, (c) UMRC2 and (d) UMRC3. *Gray bars*, SV40-luciferase reporter plasmid; *open bars*, HRE4-luciferase reporter plasmid. All expressed values are normalized to DMSO-only controls for each cell line. Experiments were performed in triplicate. Error bars represent standard error of the mean (SEM). For all panels: M, medium only; D, DMSO; or compounds, as indicated at the following concentrations: 40, 30 µM; 41, 25 µM; 76, 10 µM; 77, 5 µM.

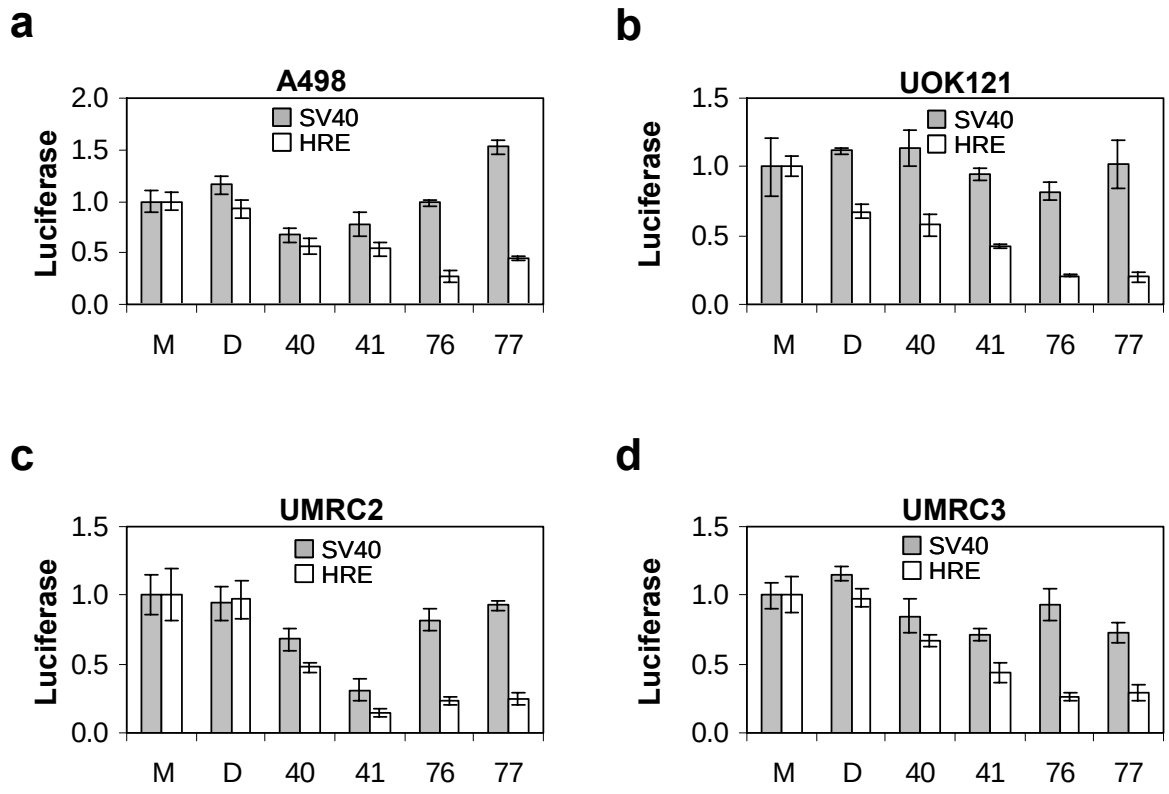

Figure S3. No Compound significantly affects HIF-2a stability as measured by blocking *de novo* protein synthesis with cyclohexamide. (a) *Effect of compound 76 on HIF-2a protein stability.* 786-O cells were treated with compound 76 for 2 days, as described for Figure 1. *De novo* protein synthesis was then halted by the addition of 10 µg/mL cycloheximide (CHx) and time points taken every hour for 4 hours. Lanes 1 and 2, PRC3 (VHL-deficient) versus WT8 (VHL-reconstituted) cells; lanes 3-8, control for HIF-2a expression without addition of cycloheximide (CHx) (lane 3, DMSO-only; lanes 4-8, 5 µM 76); lanes 9-14, HIF-2a expression following the addition of CHx (lane 9, DMSO-only, lanes 10-14, 5 µM 76 harvested at 0, 1, 2, 3 and 4 hours following the addition of CHx). B-Actin is shown for loading control. (b) *HIF-2a protein stability in 786-O cells treated with DMSO-only*. Identical experiment as described above without addition of compound 76. For panels A and B: P, PRC3; W, WT8; D, DMSO; 76, 5 µM 76. (c) *HIF-2a half-life in compound-treated 786-O cells following the addition of cycloheximide*. All compounds were tested analogously to 76 and the gels were quantified by gel densitometry. HIF-2a expression was corrected for B-Actin and normalized such that the band intensity in lane 10 was set at one. *Closed squares*, DMSO-only with no CHx (from panel B, lanes 4-8); *open squares*, DMSO-only with CHx (from panel B, lanes 10-14); *closed diamond*, 40 the presence of CHx; *open diamond*, 41 with CHx; *closed triangles*, 76 with CHx (from panel A, lanes 10-14); *open triangles*; 77 with CHx.

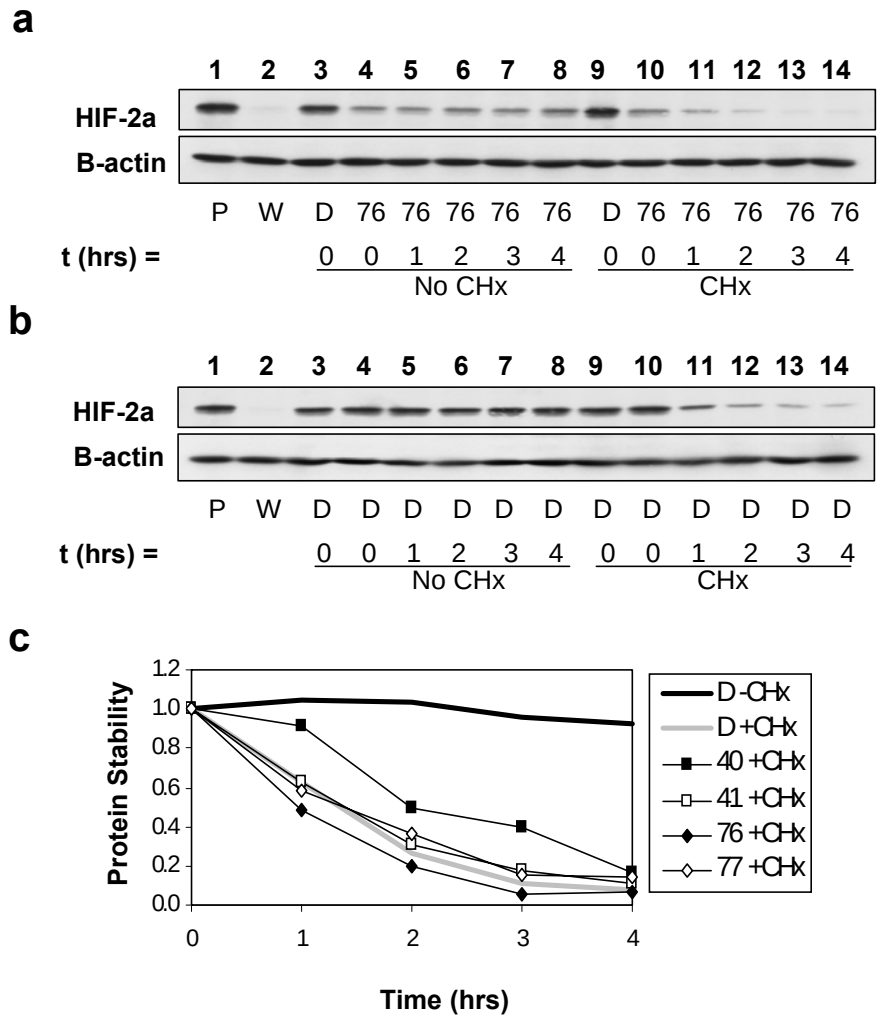

Figure S4. Compounds decrease HIF-2a mRNA translation (presentation of the whole gel). Cells were treated with compound as described in Figure 1 and ^{35}S-methionine pulse label immunoprecipitation was performed as described in Experimental Procedures. For HIF-2a immunoprecipitations, (-) indicates anti-HA control IP, (+) indicates IP with anti-HIF-2a antibody. Loading control is a representative section of the autoradiograph in which a 1:1000 dilution of the lysate was directly loaded. M, medium only; D, DMSO; compound numbers, as indicated at the following concentrations: 40, 30 µM; 41, 25 µM; 76, 10 µM; 77, 5 µM.

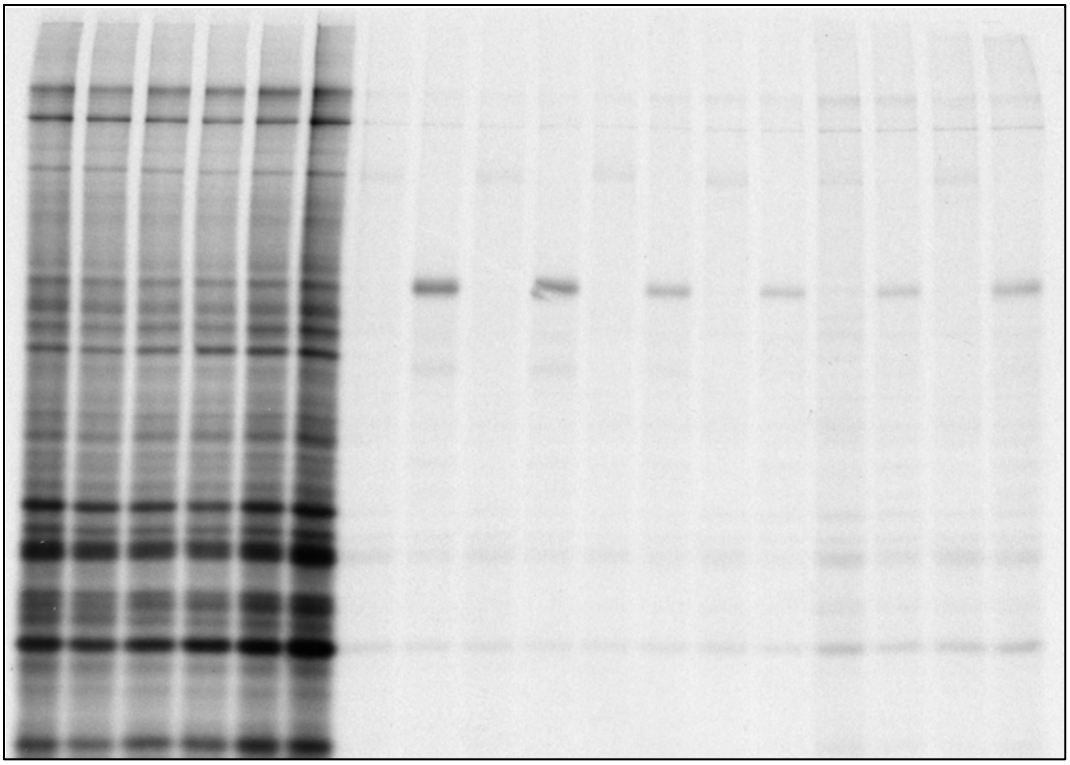

Figure S5. Compounds have no affect on HIF-2a protein stability as measured by ^{35}S-methionine pulse chase. Cells were treated as described in Figure 1 and ^{35}S-methionine pulse-chase and immunoprecipitations were performed as described in Experimental Procedures. For HIF-2a immunoprecipitations, (-) indicates anti-HA control IP, (+) indicates IP with anti-HIF-2a. Control is a 1:1000 dilution of the lysate directly loaded. M, medium only; D, DMSO; compound numbers, as indicated at the experimentally determined IC50 values. Quantification of HIF-2a protein was determined by densitometry relative to control lanes and the resulting bar graph is shown (middle). HIF-2a expression was corrected for control and normalized such that the band intensity in all t=0 lanes was set at one (top). *Closed squares*, medium only; *open squares*, DMSO; *closed diamond*, 40; *open diamond*, 41; *closed triangles*, 76; *open triangles*, 77.

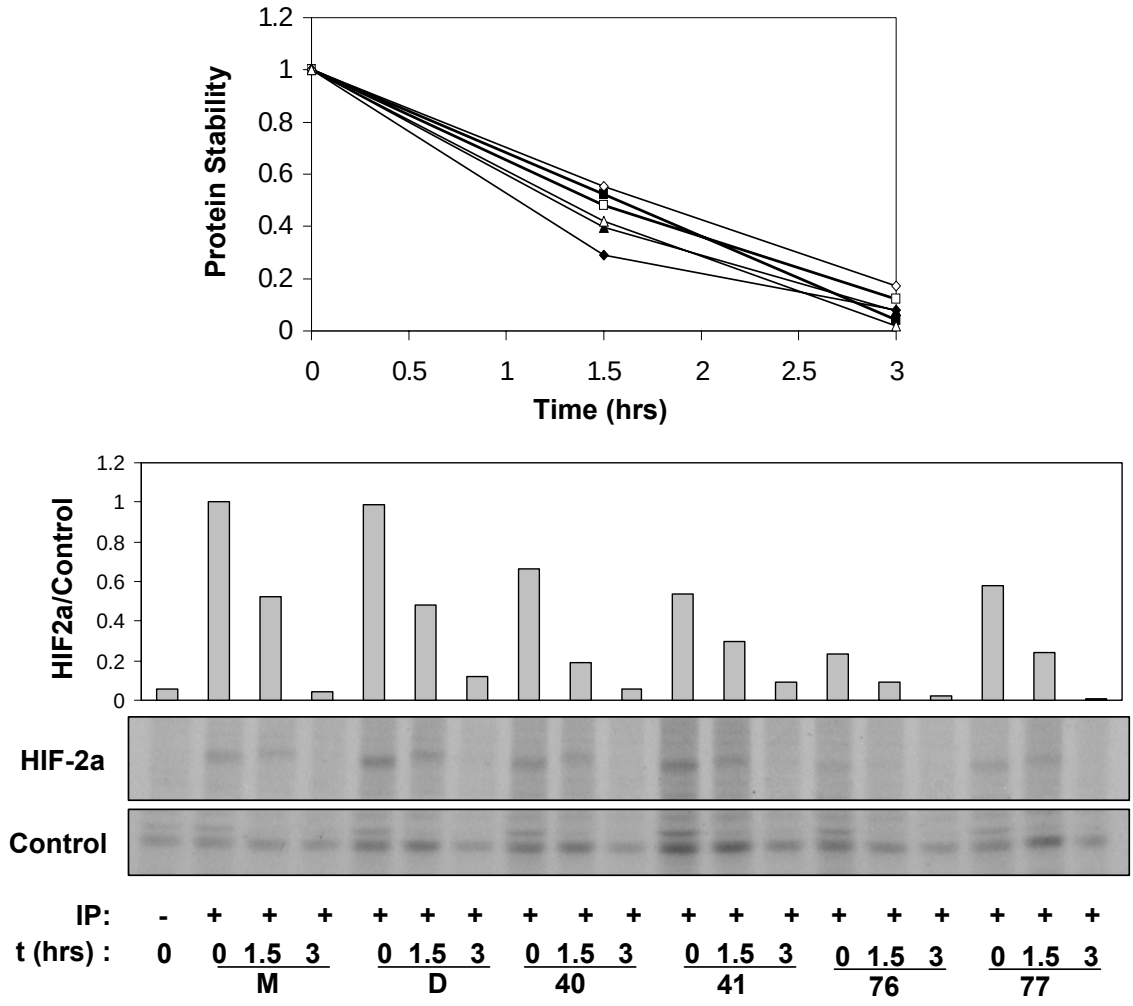

Figure S6. Comparison of compounds to low and high dose DFO by Connectivity Map. Gene-expression signatures obtained by treating 786-O cells with compound 40 (a), 41 (b), 76 (c) and 77 (d) were compared with multiple independent gene-expression profiles of MCF7 and PC3 cells treated with low (6 µM) or high (100 µM) concentrations of deferoxamine (DFO) using the Connectivity Map (www.broad.mit.edu/cmap). The barviews are constructed from 6,100 horizontal lines, each representing an individual treatment, ordered by their corresponding connectivity scores with each compound signature (+1, top; -1, bottom). All DFO instances in the dataset are colored in black. Colors applied to the remaining instances reflect the sign of their scores (green, positive; gray, null; red, negative). The rank, name [instance id], concentration, cell line and connectivity score for each DFO instance is shown. Negative score indicates degree of negative correlation.

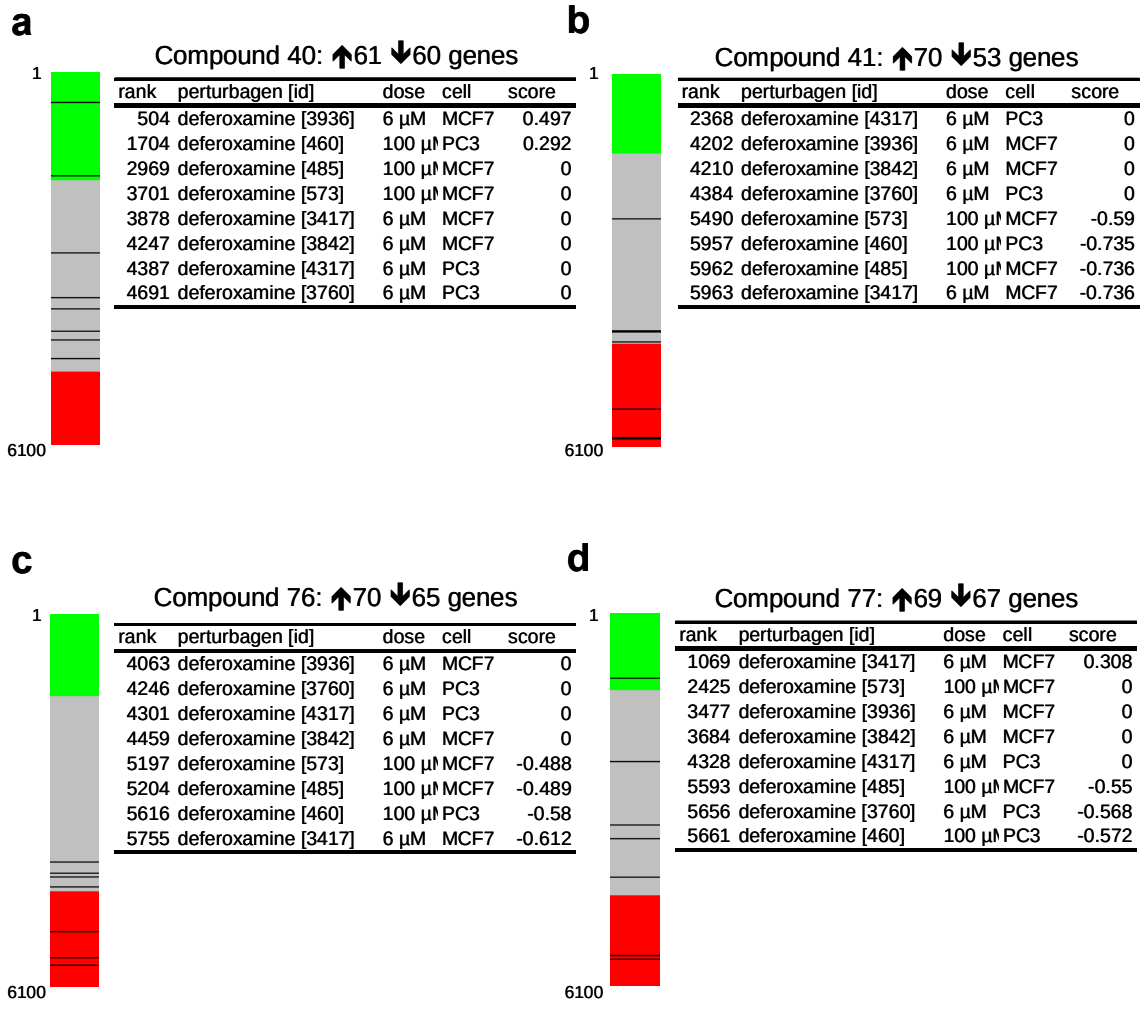

rank	perturbagen [id]	dose	cell	score
504	deferoxamine [3936]	6 µM	MCF7	0.497
1704	deferoxamine [460]	100 µM	PC3	0.292
2969	deferoxamine [485]	100 µM	MCF7	0
3701	deferoxamine [573]	100 µM	MCF7	0
3878	deferoxamine [3417]	6 µM	MCF7	0
4247	deferoxamine [3842]	6 µM	MCF7	0
4387	deferoxamine [4317]	6 µM	PC3	0
4691	deferoxamine [3760]	6 µM	PC3	0

rank	perturbagen [id]	dose	cell	score
2368	deferoxamine [4317]	6 µM	PC3	0
4202	deferoxamine [3936]	6 µM	MCF7	0
4210	deferoxamine [3842]	6 µM	MCF7	0
4384	deferoxamine [3760]	6 µM	PC3	0
5490	deferoxamine [573]	100 µM	MCF7	-0.59
5957	deferoxamine [460]	100 µM	PC3	-0.735
5962	deferoxamine [485]	100 µM	MCF7	-0.736
5963	deferoxamine [3417]	6 µM	MCF7	-0.736

rank	perturbagen [id]	dose	cell	score
4063	deferoxamine [3936]	6 µM	MCF7	0
4246	deferoxamine [3760]	6 µM	PC3	0
4301	deferoxamine [4317]	6 µM	PC3	0
4459	deferoxamine [3842]	6 µM	MCF7	0
5197	deferoxamine [573]	100 µM	MCF7	-0.488
5204	deferoxamine [485]	100 µM	MCF7	-0.489
5616	deferoxamine [460]	100 µM	PC3	-0.58
5755	deferoxamine [3417]	6 µM	MCF7	-0.612

rank	perturbagen [id]	dose	cell	score
1069	deferoxamine [3417]	6 µM	MCF7	0.308
2425	deferoxamine [573]	100 µM	MCF7	0
3477	deferoxamine [3936]	6 µM	MCF7	0
3684	deferoxamine [3842]	6 µM	MCF7	0
4328	deferoxamine [4317]	6 µM	PC3	0
5593	deferoxamine [485]	100 µM	MCF7	-0.55
5656	deferoxamine [3760]	6 µM	PC3	-0.568
5661	deferoxamine [460]	100 µM	PC3	-0.572

Figure S7. *Specific shifted band decreases in hypoxia and supershifts with IRP1 antibody*. EMSA was performed on lysates from 786-O cells subjected to 24 hours normoxia versus hypoxia. Lysates were mixed with wild-type HIF-2a IRE probe and either mock treated (No SS, for no supershift) or incubated with control, IRP1 polyclonal or IRP2 monoclonal antibodies. Control for IRP1 was preimmune sera. Control for IRP2 was purified B-Actin monoclonal. *Black arrow*: position of the shifted band, *white arrow*: position of the supershifted band.

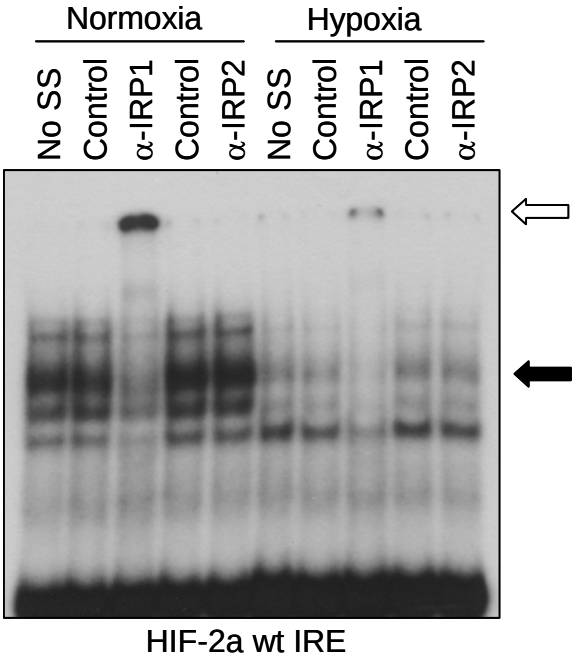

Figure S8. *Compound 76 enhances binding of endogenous IRP2 to Ferritin-L IRE*. EMSA was performed on 786-O lysates treated with D, DMSO, 10µM 76 or 150 µM DFO in normoxia or hypoxia using either the Ferritin-L or HIF-2a IRE radiolabeled probe and supershifted with either control or anti-IRP2 (2 µL UT29) antibody. *Black arrow*: position of the shifted band, *white arrow*: position of the supershifted band.

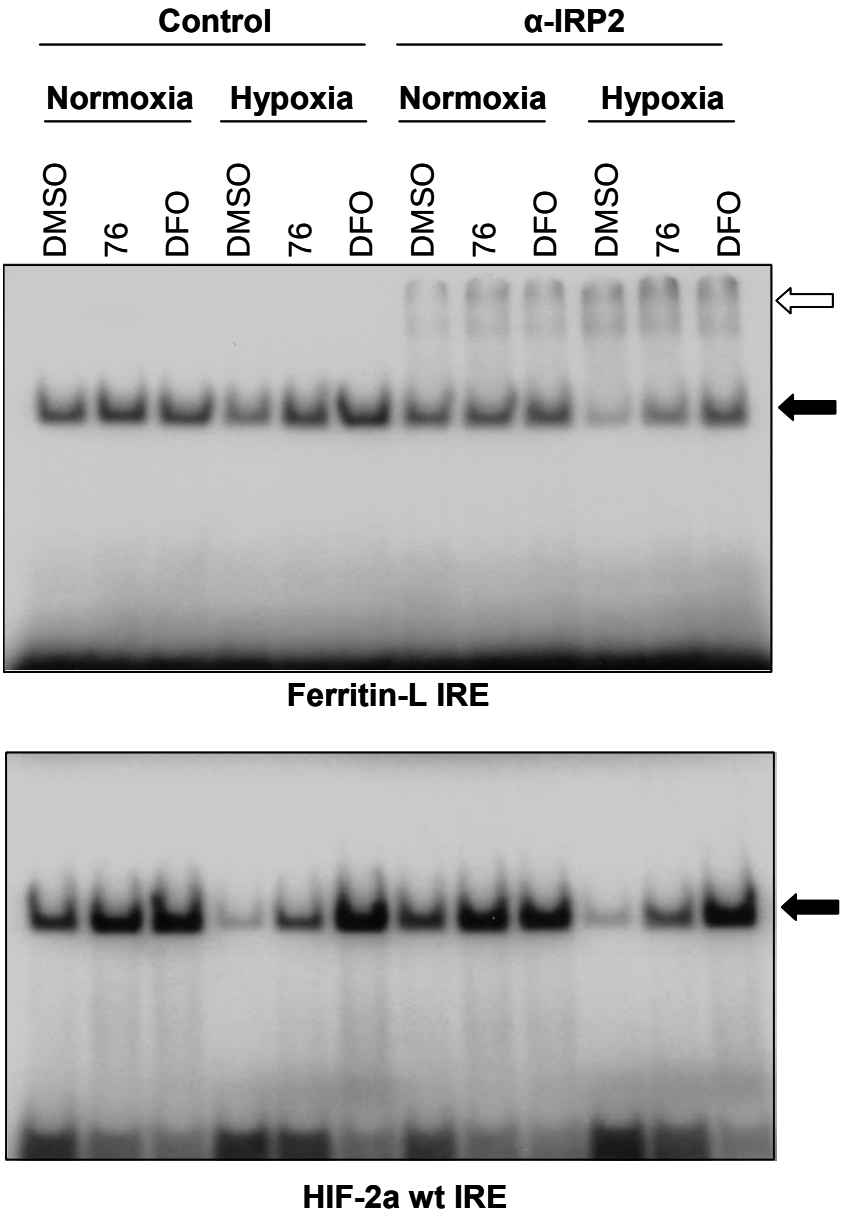

Figure S9. Compounds do not affect putative IRE in HIF-1a 5'-UTR yet indirectly suppress hypoxic induction of HIF-1a in multiple cell types. (a) *Schematic of the HIF-2a 5'-UTR Iron-responsive element (IRE) versus the putative one located in the HIF-1a 5'-UTR*. The consensus sequence of the loop and the mandatory 5' cytosine bulge are highlighted with light blue circles. (b) *The putative IRE in the HIF-1a 5'-UTR is not functional*. Duplicate plates of 786-O derived lines expressing the putative wild-type or mutant HIF-1a IRE were cultured in the presence of compound as described for Figure 1, with the exception that one set was placed at 1% oxygen for 24 hours following the first day's medium-change. Cells were treated with M, medium only; D, DMSO; or compounds, as indicated at the following concentrations: 40, 40 µM; 41, 30 µM; 76, 10 µM; 77, 5 µM. (c) *Effect of compounds on HIF-1a in CWR22R cells and HIF-1a and HIF-2a in Hep3B cells.* CWR22R or Hep3B cells were treated with compound and subjected to hypoxia as described above. B-Actin is shown for loading control. Cells were treated with M, medium only; D, DMSO; or compounds, as indicated at the following concentrations: 40, 40 µM; 41, 30 µM; 76, 20 µM; 77, 7.5 µM. Error bars represent standard error of the mean (SEM). (d) *IRP1/2 do not bind to the putative HIF-1a IRE.* EMSA was performed on 786-O lysates either left untreated (medium only, M) or treated with 150 µM DFO in normoxia or hypoxia using either the HIF-1a or HIF-2a IRE radiolabeled probe. *Black arrow*: position of the shifted band.

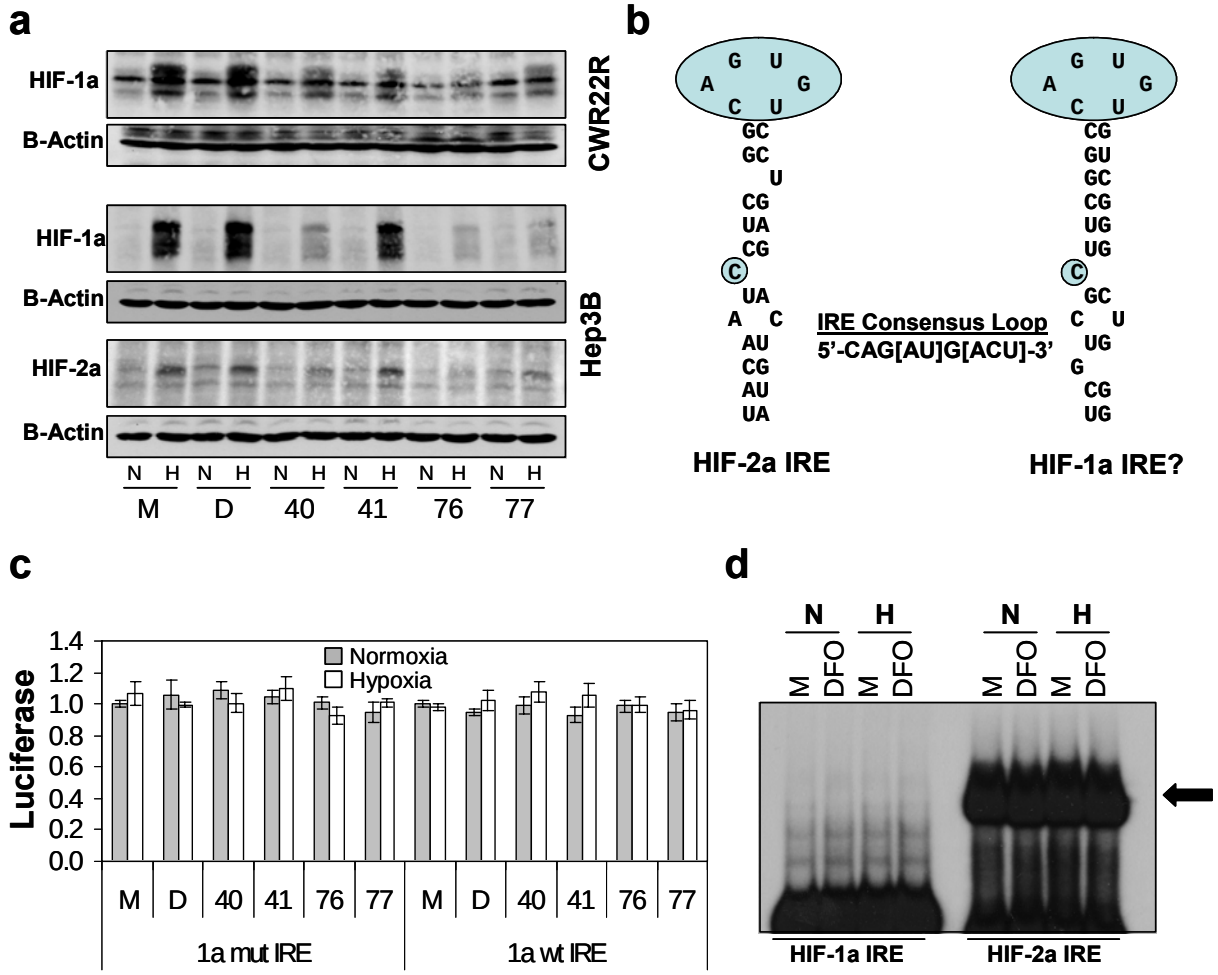

Table S1. Identified HIF inhibitor compounds.

Name	Full Chemical Name
20	3-(2,5-diethoxyphenyl)-1-(2-thienyl)-2-propen-1-one
37	N^2-(4-bromo-3-nitrobenzoyl)leucinamide
39	2-bromo-N-(2-methoxyphenyl)propanamide
40	5-(dimethylamino)-2-methyl-1-phenyl-1-penten-3-one hydrochloride
41	4-hydroxy-3-[3-(2-hydroxy-5-methoxyphenyl)acryloyl]-6-methyl-2H-pyran-2-one
42	6-(1,3-dioxo-1H-benzo[de]isoquinolin-2(3H)-yl)-N-hydroxyhexanamide
76	methyl 3-{2-[cyano(methylsulfonyl)methylene]hydrazino}thiophene-2-carboxylate
77	4-[(2,2-dimethyl-4-oxo-3,4-dihydro-2H-thiin-6-yl)thio]-3-nitrobenzonitrile

Table S2. Regulation of HIF and VHL target genes by identified compounds.

Gene set	Description	40	41	76	77
PRC3, VHL null	Markers of PRC3 cells compared to WT8 cells	NES: -3.50 p < .001	NES*: -2.98 p < .001	NES: -3.15 p < .001	NES: -3.15 p < .001
Staller, VHL null	Markers of VHL null cells compared to VHL WT cells	NES: -2.48 p < .001	NES: -2.42 p < .001	NES: -2.45 p < .001	NES: -2.45 p < .001
Schofield, HIF	Validated HIF-regulated genes as reviewed by Schofield et al.	NES: -1.65 p < .001	NES: -1.62 p = .005	NES: -1.78 p = .002	NES: -1.78 p = .002
WT8, VHL WT	Markers of WT8 cells compared to PRC3 cells	NES: -1.86 p < .001	NES: 1.58 p < .007	NES: 1.88 p < .001	NES: 1.88 p < .001
Staller, VHL WT	Markers of VHL WT cells compared to VHL null cells	NES: -1.75 p < .001	NES: 1.62 p < .001	NES: 1.53 p = .002	NES: 1.53 p = .002

* Using the GSEA algorithm, normalized enrichment scores (NES) was calculated for each gene set. A negative NES indicates downregulation of the set of genes by the compound, and a positive score indicates upregulation. Statistical significance was determined by permutation testing.

Table S3. Published HIF inhibitor compounds.

Name	Method of Identification	Mechanism of HIF inhibtion	Biological Activities	Ref.
Chemotin	HTS-p300-HIF interaction	p300-HIF interaction	tumor suppression	(Kung et al., 2004)
Topotecan	HTS- HRE-glioma cell line	HIF translation	VEGF decrease	(Rapisarda et al., 2002)
103D5R	HTS-HRE-glioma cell line	HIF translation	Decreases HIF tested target genes	(Tan et al., 2005)
YC-1	Direct Testing	HIF protein levels	VEGF decrease/tumor suppression	(Yeo et al., 2003)
GL331	Direct testing	Protein levels	Inhibits HUVEC proliferation	(Chang et al., 2003)
Geldanamycin	Direct testing	HSP90 inhibitor-HIF half life	Tumor suppression	(Mabjeesh et al., 2002)
2-ME2	Direct testing	Post-transcriptional	Inhibits HUVEC proliferation	(Mabjeesh et al., 2003)
Bisphenol	Direct testing	HIF degradation	No report	(Kubo et al., 2004)
Berberine	Direct testing	HIF degradation	No report	(Lin et al., 2004)
PX-478	Thioredoxin inhibitor	Unknown	Tumor suppression	(Welsh et al., 2004)
PX-12	Thioredoxin inhibitor	Unknown	Tumor suppression	(Welsh et al., 2004)

Table S4. Plasmids used in this study.

Plasmid	Description	Ref.
pGL3 basic	Promoterless luciferase expression vector	Promega
pGL3 promoter	SV40-luciferase expression vector	Promega
pGL3::HIF2p	1000nt HIF-2a promoter PCR fragment cloned into pGL3 basic vector (cut *NheI/HindIII*)	This work
pGL3::HIF2p-UTR	1000nt HIF-2a promoter with 5'-UTR PCR fragment cloned into pGL3 basic (cut *NheI/HindIII*)	This work
pGL3::SV-UTR	SV40-luciferase vector with HIF-2a 5'-UTR (cut *NcoI* and screened for orientation)	This work
pGL3::HRE1	1xHRE-luciferase made from pGLH3 basic vector (cut *NheI*/*XhoI*)[a]	This work
pGL3::HRE2	2xHRE-luciferase made from pGLH3 basic vector (cut *MluI*/*XhoI*)[a]	This work
pGL3::HRE3	3xHRE-luciferase made from pGLH3 basic vector (cut *SacI*/*XhoI*)[a]	This work
pGL3::HRE4	4xHRE-luciferase made from pGLH3 basic vector (cut *KpnI*/*XhoI*)[a]	This work
pGL3::HIF2p-UTR1	1-100 nt HIF-2a 5'-UTR PCR fragment cloned into pGL3::HIF2p (cut *HindIII/NcoI*)	This work
pGL3::HIF2p-UTR3	100-200 nt HIF-2a 5'-UTR PCR fragment cloned into pGL3::HIF2p (cut *HindIII/NcoI*)	This work
pGL3::HIF2p-UTR5	200-300 nt HIF-2a 5'-UTR PCR fragment cloned into pGL3::HIF2p (cut *HindIII/NcoI*)	This work
pGL3::HIF2p-UTR10	1-250 nt HIF-2a 5'-UTR PCR fragment cloned into pGL3::HIF2p (cut *HindIII/NcoI*)	This work
pGL3::HIF2p-UTR12	250-488 nt HIF-2a 5'-UTR PCR fragment cloned into pGL3::HIF2p (cut *HindIII/NcoI*)	This work
pGL3::HIF2p-UTR13	1-488 nt (full length) HIF-2a 5'-UTR PCR fragment cloned into pGL3::HIF2p (cut *HindIII/NcoI*)	This work
pGL3::HIF2p-UTR16	50-100 nt HIF-2a 5'-UTR fragment generated using annealed oligos with overhaning *HindIII/NcoI* sites cloned into pGL3::HIF2p (cut *HindIII/NcoI*)	This work
pGL3::HIF2p-UTR17	Mutant 50-100 nt HIF-2a 5'-UTR fragment generated using annealed oligos with overhaning *HindIII/NcoI* sites cloned into pGL3::HIF2p (cut *HindIII/NcoI*)) in which CAGTGT of the IRE stem loop is changed to CAAAGT	This work
pGL3::HIF2p-1aUTR16	35-86 nt HIF-1a 5'-UTR fragment generated using annealed oligos with overhaning *HindIII/NcoI* sites cloned into pGL3::HIF2p (cut *HindIII/NcoI*)	This work
pGL3::HIF2p-1aUTR17	Mutant 35-86 nt HIF-1a 5'-UTR fragment generated using annealed oligos with overhaning *HindIII/NcoI* sites cloned into pGL3::HIF2p (cut *HindIII/NcoI*)) in which CAGTGT of the IRE stem loop is changed to CAAAGT	This work
pcDNA3.1	Mammalian expression vector	Invitrogen
pcDNA3.1::SV40	SV40-luciferase from pGL3 promoter (cut *NotI*[b]/*XbaI*) subcloned into pcDNA3.1 (cut *MluI*[b]/*XbaI*)	This work
pcDNA3.1::HRE4	4xHRE-luciferase from pGLH4 (cut *NotI*[b]/*XbaI*) subcloned into pcDNA3.1 (cut *MluI*[b]/*XbaI*)	This work
pcDNA3.1::HIF2p	HIF-2a promoter-luciferase from pGL3::HIF2p (cut *NotI*[b]/*XbaI*) subcloned into pcDNA3.1 (cut *MluI*[b]/*XbaI*)	This work
pcDNA3.1::HIF2p-UTR	HIF-2a promoter-UTR-luciferase from pGL3::HIF2p-UTR (cut *BglI*[b]/*XbaI*) subcloned into pcDNA3.1 (cut *MluI*[b]/*XbaI*)	This work
pcDNA3.1::SV40-UTR	SV40-UTR-luciferase from pGL3::SV-UTR (cut *NotI*[b]/*XbaI*) subcloned into pcDNA3.1 (cut *MluI*[b]/*XbaI*)	This work
pcDNA3.1::CMV	CMV-Luciferase in pcDNA3.1	This work
pcDNA3.1::CMV-SL	CMV-SL-luciferase in pcDNA3.1 (SL is a synthetic 5'-UTR with a stem loop to measure RNA helicase activity)	This work
pcDNA3.1::HIF2p-UTR1	HIF-2a promoter-UTR1-luciferase from pGL3::HIF2p-UTR1 (cut *BglI*[b]/*XbaI*) subcloned into pcDNA3.1 (cut *MluI*[b]/*XbaI*)	This work
pcDNA3.1::HIF2p-UTR3	HIF-2a promoter-UTR1-luciferase from pGL3::HIF2p-UTR3 (cut *BglI*[b]/*XbaI*) subcloned into pcDNA3.1 (cut *MluI*[b]/*XbaI*)	This work
pcDNA3.1::HIF2p-UTR5	HIF-2a promoter-UTR1-luciferase from pGL3::HIF2p-UTR5 (cut *BglI*[b]/*XbaI*) subcloned into pcDNA3.1 (cut *MluI*[b]/*XbaI*)	This work
pcDNA3.1::HIF2p-UTR10	HIF-2a promoter-UTR1-luciferase from pGL3::HIF2p-UTR10 (cut *BglI*[b]/*XbaI*) subcloned into pcDNA3.1 (cut *MluI*[b]/*XbaI*)	This work
pcDNA3.1::HIF2p-UTR12	HIF-2a promoter-UTR1-luciferase from pGL3::HIF2p-UTR12 (cut *BglI*[b]/*XbaI*) subcloned into pcDNA3.1 (cut *MluI*[b]/*XbaI*)	This work
pcDNA3.1::HIF2p-UTR16	HIF-2a promoter-UTR1-luciferase from pGL3::HIF2p-UTR16 (cut *BglI*[b]/*XbaI*) subcloned into pcDNA3.1 (cut *MluI*[b]/*XbaI*)	This work
pcDNA3.1::HIF2p-UTR17	HIF-2a promoter-UTR1-luciferase from pGL3::HIF2p-UTR17 (cut *BglI*[b]/*XbaI*) subcloned into pcDNA3.1 (cut *MluI*[b]/*XbaI*)	This work
pcDNA3.1::HIF2p-1aUTR16	HIF-2a promoter-UTR1-luciferase from pGL3::HIF2p-UTR16 (cut *BglI*[b]/*XbaI*) subcloned into pcDNA3.1 (cut *MluI*[b]/*XbaI*)	This work
pcDNA3.1::HIF2p-1aUTR17	HIF-2a promoter-UTR1-luciferase from pGL3::HIF2p-UTR17 (cut *BglI*[b]/*XbaI*) subcloned into pcDNA3.1 (cut *MluI*[b]/*XbaI*)	This work
pcDNA3.1::UTR16 probe	pGL3::HIF2p-UTR16 (cut *HindIII/XbaI*) cloned into pcDNA3.1 (cut *HindIII/XbaI*) to maintain T7 promoter for EMSA probe	This work
pcDNA3.1::UTR17 probe	pGL3::HIF2p-UTR17 (cut *HindIII/XbaI*) cloned into pcDNA3.1 (cut *HindIII/XbaI*) to maintain T7 promoter for EMSA probe	This work
pRL-SV40	Control SV40-Renilla luciferase construct used to normalize transient transfections	Promega
pIRESpuro	Mammalian Internal Ribosomal Entry Site (IRES) expression vector	BD Biosciences
pIRESpuro::HIF-2a(P531A)	Degradation-resistant HIF-2a(P531A) mutant	This work
pIREShygro	Mammalian Internal Ribosomal Entry Site (IRES) expression vector	BD Biosciences
pIREShygro::dnHIFA	Dominant negative HIF-2a construct lacking transactivation domain (aa's 1-517)	This work

pIREShygro::dnHIFB	Dominant negative HIF-2a construct lacking transactivation domain including N-terminus NLS sequence (aa's 1-517 fused to aa's 738-741)	This work
pIREShygro::dnHIFC	Dominant negative HIF-2a construct lacking N- and C-terminal transactivation domains (aa's 530-682 and 828-870)	This work
pRC/CMV	Mammalian expression vector	(Iliopoulos et al., 1995)
pRC/CMV::VHL30	VHL30 cloned into pRC/CMV	(Iliopoulos et al., 1995)
pTUIIa$^-$	Stable hairpin shRNAi expression vector	(Zimmer et al., 2004)
pTUIIa$^-$::HIF-2a	Stable hairpin shRNAi expression vector targeting HIF-2a	(Zimmer et al., 2004)
pLentiLox3.7puro	pLentiLox3.7 vector conferring puromycin resistance	J. Rocco, unpublished
pLentiLox3.7hygro	pLentiLox3.7 vector conferring hygromycin resistance	J. Rocco, unpublished
pLentiLox3.7blasti	pLentiLox3.7 vector conferring blasticidin resistance	J. Rocco, unpublished
pLentiLox3.7puro::IRP1-15	The following oligos were annealed and ligated in to pLentiLox3.7puro (cut *XhoI/HpaI*): 5'-TGACCTTCCAGGCTGTCATGAGGTTCAAGAGACCTCATGACAGCCTGGAAGGTCTTTTTTC-3' 5'-TCGAGAAAAAAGACCTTCCAGGCTGTCATGAGGTCTCTTGAACCTCATGACAGCCTGGAAGGTCA-3'	This work
pLentiLox3.7hygro::IRP1-14	The following oligos were annealed and ligated in to pLentiLox3.7hygro (cut *XhoI/HpaI*): 5'-TGCCATCACACAGGGAGACCTTGTTCAAGAGACAAGGTCTCCCTGTGTGATGGCTTTTTTC-3' 5'-TCGAGAAAAAAGCCATCACACAGGGAGACCTTGTCTCTTGAACAAGGTCTCCCTGTGTGATGGCA-3'	This work
pLentiLox3.7blasti::IRP2-4	The following oligos were annealed and ligated in to pLentiLox3.7blasti (cut *XhoI/HpaI*): 5'-TGGATTCTGGGGTGGGGGGTCTCTTCACCCCCCACCCCAGAATCCTTTTTTC-3' 5'-TCGAGAAAAAAGGATTCTGGGGTGGGGGGTGAAGAGACCCCCCACCCCAGAATCCA-3'	This work
pMDLG/pRRE	LentiLox3.7 helper plasmid encoding gag/pol elements	(Dull et al., 1998)
pRSV-Rev	LentiLox3.7 helper plasmid encoding Rev	(Dull et al., 1998)
pCMV-VSVG	LentiLox3.7 helper plasmid encoding envelope for viral pseudotyping	(Dull et al., 1998)

[a] HRE (5'-CCACAGTGCATACGTGGGCTCCAACAGGTCCTCTTCCCTCCCATGCA-3') cloned into pGL3 basic vector using 4 sets of annealed oligos with overhanging *Kpn1, SacI, MluI, NheI* or *XhoI* sites. Final product was *KpnI*-HRE4-*SacI*-HRE3-*MluI*-HRE2-*NheI*-HRE1-*XhoI* where *SacI, MluI* and *NheI* sites were destroyed.

[b] site blunt-ended following restriction digest using T7 polymerase

Table S5. Cell lines used in this study.

Cell line	Description	Ref.
U2OS	Osteosarcoma cell line used for transient transfection experiments	(Ponten and Saksela, 1967)
Hep3B	Hepatoblastoma	(Aden et al., 1979)
786-O	$VHL^{-/-}$ Renal Clear Cell Carcinoma (RCC)	(Williams et al., 1978)
WT8	786-O derived clone stably transfected with pRC/CMV::VHL30, *neo*^{r}	(Iliopoulos et al., 1995)
PRC3	Matched vector only control for WT8 cells, *neo*^{r}	(Iliopoulos et al., 1995)
7TR1	786-O derived clone stably transfected with pTUIIa$^-$::HIF-2a targeting shRNAi, *blasti*^{r}	(Zimmer et al., 2004)
7TV1	Matched vector only control for 7TR1 cells, *blasti*^{r}	(Zimmer et al., 2004)
7H4	786-O derived clone stably transfected with pcDNA3.1::HRE4, *neo*^{r}	This work
7SV	786-O derived clone stably transfected with pDNA3.1::SV40, *neo*^{r}	This work
7SV-UTR	786-O derived polyclonal line stably transfected with pDNA3.1::SV40-UTR, *neo*^{r}	This work
7H2P2	786-O derived polyclonal line stably transfected with pcDNA3.1::HIF2p, *neo*^{r}	This work
7H2P3	786-O derived polyclonal line stably transfected with pcDNA3.1::HIF2p-UTR, *neo*^{r}	This work
7CMV	786-O derived polyclonal line stably transfected with pcDNA3.1::CMV, *neo*^{r}	(Yang et al., 2004)
7H2P2-UTR1	786-O derived polyclonal line stably transfected with pcDNA3.1::HIF2p-UTR1, *neo*^{r}	This work
7H2P2-UTR3	786-O derived polyclonal line stably transfected with pcDNA3.1::HIF2p-UTR3, *neo*^{r}	This work
7H2P2-UTR5	786-O derived polyclonal line stably transfected with pcDNA3.1::HIF2p-UTR5, *neo*^{r}	This work
7H2P2-UTR10	786-O derived polyclonal line stably transfected with pcDNA3.1::HIF2p-UTR10, *neo*^{r}	This work
7H2P2-UTR12	786-O derived polyclonal line stably transfected with pcDNA3.1::HIF2p-UTR12 *neo*^{r}	This work
7H2P2-UTR13	786-O derived polyclonal line stably transfected with pcDNA3.1::HIF2p-UTR13 *neo*^{r}	This work
7H2P2-UTR16	786-O derived polyclonal line stably transfected with pcDNA3.1::HIF2p-UTR16, *neo*^{r}	This work
7H2P2-UTR17	786-O derived polyclonal line stably transfected with pcDNA3.1::HIF2p-UTR17, *neo*^{r}	This work
7H2P2-1aUTR16	786-O derived polyclonal line stably transfected with pcDNA3.1::HIF2p-1aUTR16, *neo*^{r}	This work
7H2P2-1aUTR17	786-O derived polyclonal line stably transfected with pcDNA3.1::HIF2p-1aUTR17, *neo*^{r}	This work
7CMV-SL	786-O derived polyclonal line stably transfected with pcDNA3.1::CMV-SL, *neo*^{r}	(Yang et al., 2004)
7UTR16 v.o.	7H2P2-UTR16 line infected with pLentiLox3.7puro, pLentiLox3.7hygro and pLentiLox3.7blasti	This work
7UTR16 IRP1 k.d.	7H2P2-UTR16 line infected with pLentiLox3.7puro::IRP1-15, pLentiLox3.7hygro::IRP1-14 and pLentiLox3.7blasti	This work
7UTR16 IRP2 k.d.	7H2P2-UTR16 line infected with pLentiLox3.7puro, pLentiLox3.7hygro and pLentiLox3.7blasti::IRP2-4	This work
7UTR16 IRP1/2 k.d.	7H2P2-UTR16 line infected with pLentiLox3.7puro::IRP1-15, pLentiLox3.7hygro::IRP1-14 and pLentiLox3.7blasti::IRP2-4	This work
A498	$VHL^{-/-}$ RCC	(Giard et al., 1973)
A-H4	A498 derived polyclonal line stably transfected with pcDNA3.1::HRE4, *neo*^{r}	This work
A-SV	A498 derived polyclonal line stably transfected with pDNA3.1::SV40, *neo*^{r}	This work
UMRC2	$VHL^{-/-}$ RCC	(Grossman et al., 1985)
U2-H4	UMRC2 derived polyclonal line stably transfected with pcDNA3.1::HRE4, *neo*^{r}	This work
U2-SV	UMRC2 derived polyclonal line stably transfected with pDNA3.1::SV40, *neo*^{r}	This work
UMRC3	$VHL^{-/-}$ RCC	(Grossman et al., 1985)
U3-H4	UMRC3 derived polyclonal line stably transfected with pcDNA3.1::HRE4, *neo*^{r}	This work
U3-SV	UMRC3 derived polyclonal line stably transfected with pDNA3.1::SV40, *neo*^{r}	This work
UOK121	$VHL^{-/-}$ RCC	(Herman et al., 1994)
UK-H4	UOK121 derived polyclonal line stably transfected with pcDNA3.1::HRE4, *neo*^{r}	This work
UK-SV	UOK121 derived polyclonal line stably transfected with pDNA3.1::SV40, *neo*^{r}	This work

neo^r, neomycin/G418 resistant; *blasti*^{r}, blasticidin resistant

Supplemental References

Aden, D. P., Fogel, A., Plotkin, S., Damjanov, I., and Knowles, B. B. (1979). Controlled synthesis of HBsAg in a differentiated human liver carcinoma-derived cell line. Nature *282*, 615-616.

Chang, H., Shyu, K. G., Lee, C. C., Tsai, S. C., Wang, B., Hsien Lee, Y., and Lin, S. (2003). GL331 inhibits HIF-1alpha expression in a lung cancer model. Biochem Biophys Res Commun *302*, 95-100.

Dull, T., Zufferey, R., Kelly, M., Mandel, R. J., Nguyen, M., Trono, D., and Naldini, L. (1998). A third-generation lentivirus vector with a conditional packaging system. J Virol *72*, 8463-8471.

Giard, D. J., Aaronson, S. A., Todaro, G. J., Arnstein, P., Kersey, J. H., Dosik, H., and Parks, W. P. (1973). In vitro cultivation of human tumors: establishment of cell lines derived from a series of solid tumors. J Natl Cancer Inst *51*, 1417-1423.

Grossman, H. B., Wedemeyer, G., and Ren, L. Q. (1985). Human renal carcinoma: characterization of five new cell lines. J Surg Oncol *28*, 237-244.

Herman, J. G., Latif, F., Weng, Y., Lerman, M. I., Zbar, B., Liu, S., Samid, D., Duan, D.-S. R., Gnarra, J. R., Linhean, W. M., and Baylin, S. B. (1994). Silencing of the VHL tumor-suppressor gene by DNA methylation in renal carcinoma. Proc Natl Acad Sci (USA) *91*, 9700-9704.

Iliopoulos, O., Kibel, A., Gray, S., and Kaelin, W. G. (1995). Tumor Suppression by the Human von Hippel-Lindau Gene Product. Nature Medicine *1*, 822-826.

Kubo, T., Maezawa, N., Osada, M., Katsumura, S., Funae, Y., and Imaoka, S. (2004). Bisphenol A, an environmental endocrine-disrupting chemical, inhibits hypoxic response via degradation of hypoxia-inducible factor 1alpha (HIF-1alpha): structural requirement of bisphenol A for degradation of HIF-1alpha. Biochem Biophys Res Commun *318*, 1006-1011.

Kung, A. L., Zabludoff, S. D., France, D. S., Freedman, S. J., Tanner, E. A., Vieira, A., Cornell-Kennon, S., Lee, J., Wang, B., Wang, J., *et al.* (2004). Small molecule blockade of transcriptional coactivation of the hypoxia-inducible factor pathway. Cancer Cell *6*, 33-43.

Lin, S., Tsai, S. C., Lee, C. C., Wang, B. W., Liou, J. Y., and Shyu, K. G. (2004). Berberine inhibits HIF-1alpha expression via enhanced proteolysis. Mol Pharmacol *66*, 612-619.

Mabjeesh, N. J., Escuin, D., LaVallee, T. M., Pribluda, V. S., Swartz, G. M., Johnson, M. S., Willard, M. T., Zhong, H., Simons, J. W., and Giannakakou, P. (2003). 2ME2 inhibits tumor growth and angiogenesis by disrupting microtubules and dysregulating HIF. Cancer Cell *3*, 363-375.

Mabjeesh, N. J., Post, D. E., Willard, M. T., Kaur, B., Van Meir, E. G., Simons, J. W., and Zhong, H. (2002). Geldanamycin induces degradation of hypoxia-inducible factor 1alpha protein via the proteosome pathway in prostate cancer cells. Cancer Res *62*, 2478-2482.

Ponten, J., and Saksela, E. (1967). Two established in vitro cell lines from human mesenchymal tumours. Int J Cancer *2*, 434-447.

Rapisarda, A., Uranchimeg, B., Scudiero, D. A., Selby, M., Sausville, E. A., Shoemaker, R. H., and Melillo, G. (2002). Identification of small molecule inhibitors of hypoxia-inducible factor 1 transcriptional activation pathway. Cancer Res *62(15):*, 4316-4324.

Tan, C., de Noronha, R. G., Roecker, A. J., Pyrzynska, B., Khwaja, F., Zhang, Z., Zhang, H., Teng, Q., Nicholson, A. C., Giannakakou, P., *et al.* (2005). Identification of a novel small-molecule inhibitor of the hypoxia-inducible factor 1 pathway. Cancer Res *65*, 605-612.

Welsh, S., Williams, R., Kirkpatrick, L., Paine-Murrieta, G., and Powis, G. (2004). Antitumor activity and pharmacodynamic properties of PX-478, an inhibitor of hypoxia-inducible factor-1alpha. Mol Cancer Ther *3*, 233-244.
Williams, R. D., Elliott, A. Y., Stein, N., and Fraley, E. E. (1978). In vitro cultivation of human renal cell cancer. II. Characterization of cell lines. In Vitro *14*, 779-786.
Yang, H. S., Cho, M. H., Zakowicz, H., Hegamyer, G., Sonenberg, N., and Colburn, N. H. (2004). A novel function of the MA-3 domains in transformation and translation suppressor Pdcd4 is essential for its binding to eukaryotic translation initiation factor 4A. Mol Cell Biol *24*, 3894-3906.
Yeo, E. J., Chun, Y. S., Cho, Y. S., Kim, J., Lee, J. C., Kim, M. S., and Park, J. W. (2003). YC-1: a potential anticancer drug targeting hypoxia-inducible factor 1. J Natl Cancer Inst *95*, 516-525.
Zimmer, M., Doucette, D., Siddiqui, N., and Iliopoulos, O. (2004). Inhibition of Hypoxia Inducible Factor is Sufficient for Growth Suppression of VHL-/- Tumors. Mol Cancer Res *2*, 89-95.